Preparation, characterization and catalyst application of ternary interpenetrating networks of poly 4-methyl vinyl pyridinium hydroxide–SiO$_2$–Al$_2$O$_3$

Roozbeh Javad Kalbasi *, Majid Kolahdoozan *, Sedigheh Mozafari Vanani

Department of Chemistry, Shahreza Branch, Islamic Azad University, 311-86145 Shahreza, Isfahan, Iran

ABSTRACT

In this work, Al$_2$O$_3$ was mixed with SiO$_2$ and poly 4-vinylpyridine by the sol–gel method in order to make a composite which is used as a heterogeneous basic catalyst for Knoevenagel condensation reaction. The physical and chemical properties of the composite catalyst were investigated by XRD, FT-IR, TG, BET and SEM techniques. The catalytic performance of each material was determined for the Knoevenagel condensation reaction between carbonyl compound and malononitrile. The reactions were performed in solvent-free conditions and the product was obtained in high yield and purity after a simple work-up. The effects of the amount of catalyst, amount of monomer for the synthesis of composite and recyclability of the heterogeneous composite were investigated. The composite catalyst used for this synthetically useful transformation showed considerable level of reusability besides very good activity.

© 2011 Elsevier Inc. All rights reserved.

1. Introduction

Homogeneous catalysts are soluble species that are usually very active and selective. Their syntheses are guided by molecular design principles, but are often difficult to use in industry. They suffer from high costs associated with separating them from products and consequential difficulties in recycling. The development of heterogeneous catalysts to replace homogeneous systems for the production of a wide range of chemicals is motivated by several potential advantages such as easier separation of the catalyst from the reaction medium, greater catalyst stability, improved regenerability, eco-benignity, and fitting the concepts of "green chemical process". They can be designed to give higher activity, selectivity and longer catalyst lifetimes [1–4].

Polymer-inorganic hybrid materials obtained by combining organic polymers and inorganic compounds at nano or molecular order are expected to be the original material which exhibit high performance in all properties. Both pure organic polymer and pure inorganic materials have their own advantages and disadvantages. The organic polymer materials exhibit excellent flexibility, toughness, moldability and adhesiveness, but their heat-resistance properties are inferior to those of inorganic materials. On the other hand, inorganic materials show high elastic modulus, heat resistance, corrosiveness, weather resistance, solvent resistance and mechanical strength. However, they are very brittle and their moldability is very poor. Therefore, the combination of inorganic and organic moieties in a single-phase material can lead us to tailor the mechanical, electrical and optical properties with respect to numerous applications [5–8] such as catalysis, adsorption, separation, drug delivery and sensing [9–17].

Sol–gel technology, which is mainly based on inorganic polymerization reactions, is an important way to synthesize organic–inorganic hybrid materials because of its unique low temperature processing characteristic providing opportunities to let organic and inorganic phases mix well and incorporate with each other at temperatures under which the organic phase can survive. Since the last few decades, the preparation, characterization and application of those organic–inorganic hybrid materials based on the sol–gel process have been the fast growing research field in materials science [5–9,18–20].

Knoevenagel condensation is one of the well-known reactions in organic chemistry right from the syntheses of small molecules to the elegant intermediates of anti-hypertensive drugs and calcium antagonists. It is generally catalyzed by weak bases like primary, secondary, tertiary amines, ammonium or ammonium salts under homogeneous conditions. In the last decade, a wide range of catalysts, such as MgO [21], NbCl$_5$ [22], MgF$_2$ [23] Na$_2$CaP$_2$O$_7$ [24] chitosan [25], ionic liquids containing imidazole [26] or guanidinium group [27], have been employed to catalyze

* Corresponding authors. Fax: +98 321 3213103.
  E-mail addresses: rkalbasi@iaush.ac.ir (R.J. Kalbasi),
kolahdoozan@iaush.ac.ir (M. Kolahdoozan).

this reaction. However, the use of such catalysts is associated with environmental pollution. In the recent years, solid basic catalysts have received an increased attention as they facilitate a variety of organic reactions that take place via carbanionic intermediates [28–39].

In this paper, we report the synthesis of poly 4-methyl vinyl pyridinium hydroxide–SiO$_2$–Al$_2$O$_3$ (P4MVPH–SiO$_2$–Al$_2$O$_3$) by the in-situ polymerization of 4-vinylpyridine (4VP) in the presence of aluminum isopropoxide and tetraethyl orthosilicate (TEOS), subsequent quaternization with methyl iodide and ion exchange occurs with NaOH. The novelty of this procedure is at easy preparation together with using inexpensive materials. The basic property of this new polymeric inorganic catalyst was tested for Knoevenagel condensation of various aldehydes with malononitrile in solvent-free conditions. The composite could be easily recovered by simple washing and filtration and reused up to 5 times without significant loss in its catalytic activity.

2. Experimental

2.1. Instruments and characterization

The catalyst was characterized by X-ray diffraction (Bruker D8ADVANCE, Cu $K\alpha$ radiation), FT-IR spectroscopy (Nicolet 400D in KBr matrix in the range of 4000–400 cm^{-1}), BET specific surface areas and BJH pore size distribution (Series BEL SORP 18, at 77 K), thermal analyzer TGA (Setaram Labsys TG (STA) in temperature 30–700 °C and heating rate of 10 °C/min in N$_2$ atmosphere) and SEM (Philips, XL30, SE detector).

The products were characterized by ^{1}H and ^{13}C NMR spectra (Bruker DRX-500 Avance spectrometer at 500.13 and 125.47 MHz, respectively), GC (Agilent 6820 equipped with a FID detector) and GC–MS (Agilent 6890). Melting points were measured on an Electrothermal 9100 apparatus and they were uncorrected. All the products were known compounds and they were characterized by FTIR, ^{1}H NMR and ^{13}C NMR. All melting points were compared satisfactorily with those reported in the literature.

2.2. Catalyst preparation

2.2.1. Preparation of the 4-methyl vinyl pyridinium hydroxide–SiO$_2$–Al$_2$O$_3$ composite by in-situ polymerization

In the first step, poly 4-vinyl pyridine–SiO$_2$–Al$_2$O$_3$ was prepared by in-situ method. Aluminum isopropoxide (1.84 g, 9 mmol) was dissolved in n-butanol. Through this clear solution, acetyl acetone (2.06 mL, 0.02 mol), TEOS (2 mL, 8.9 mmol), 4-vinylpyridine (2 mL, 18.5 mmol) and K$_2$S$_2$O$_8$ (0.5 g, 1.84 mmol) were added under continuous stirring, and the mixture was heated to 60–70 °C. After 1 h, the solution was cooled down to room temperature and deionized water (10 mL) as the hydrolyzing agent was added slowly. The reaction mixture was left overnight to hydrolyze the alkoxides, yielding transparent gel. The obtained gel was dried at 60 °C and gave 4.2 g poly 4-vinyl pyridine–SiO$_2$–Al$_2$O$_3$ (P4VP–SiO$_2$–Al$_2$O$_3$).

In the second step, the obtained P4VP–SiO$_2$–Al$_2$O$_3$ (4.2 g), CH$_3$I (2 mL, 0.046 mol) and CH$_2$Cl$_2$ (20 mL) were added to a 50 mL round-bottomed flask. The solution was stirred with magnetic stirrer and refluxed for 6 h at 40 °C. This mixture was filtered and washed with CH$_2$Cl$_2$ (2 × 10 mL) and the precipitate was dried in air to yield poly 4-methyl vinyl pyridinium iodide–SiO$_2$–Al$_2$O$_3$ (P4MVPI–SiO$_2$–Al$_2$O$_3$).

In the third step, the aqueous solution of NaOH (0.027 mol of NaOH in 20 mL·H$_2$O) was added to the obtained P4MVPI–SiO$_2$–Al$_2$O$_3$ at room temperature. The mixture was stirred for 7.5 h. Then, it was filtered and washed sequentially with deionized

water to remove excess NaOH and was dried in room temperature to yield poly 4-methyl vinyl pyridinium hydroxide–SiO$_2$–Al$_2$O$_3$ (P4MVPH–SiO$_2$–Al$_2$O$_3$ (in-situ)) composite.

Hydroxide content of P4MVPH–SiO$_2$–Al$_2$O$_3$ composite was estimated by back titration using NaOH (0.2 N). 10 mL of HCl (0.2 N) was added to 0.05 g of this composite and stirred for 30 min. The catalyst was removed and washed successively with deionized water. The excess amount of HCl was titrated with NaOH (0.2 N) in the presence of phenol phthalein as indicator. Basic sites content of the catalyst was 4.8 mmol g^{-1}.

The procedure for preparing P4MVPH–SiO$_2$–Al$_2$O$_3$ (in-situ) is given in Scheme 1.

2.2.2. General procedure for Knoevenagel condensation reaction

The catalytic activity of P4MVPH–SiO$_2$–Al$_2$O$_3$ was tested for the Knoevenagel condensation. In a typical experiment, 1 mmol of benzaldehyde (0.10 mL), 1 mmol of malononitrile (0.07 mg) and 0.12 g of catalyst (P4MVPH–SiO$_2$–Al$_2$O$_3$) were taken in a round-bottom flask, and were stirred. The reaction was carried out under solvent-free condition at room temperature. (It should be mentioned that in the case solid aldehydes, the mixture was ground at room temperature in a glass mortar and pestle.) The progress and completion of the reaction was monitored by TLC, using n-hexane/ethyl acetate (5:1) as eluent. After 3 min of reaction, the mixture was cooled to 10 °C, for the solidification of the product. 10 ml of hot ethanol was added to the reaction mixture and the catalyst was separated from the reaction mixture by filtration. The residual solid was re-crystallized with hot ethanol (5 mL). The product was identified with ^{1}H NMR, ^{13}C NMR and FT-IR spectroscopy techniques and compared with the authentic samples.

3. Results and discussion

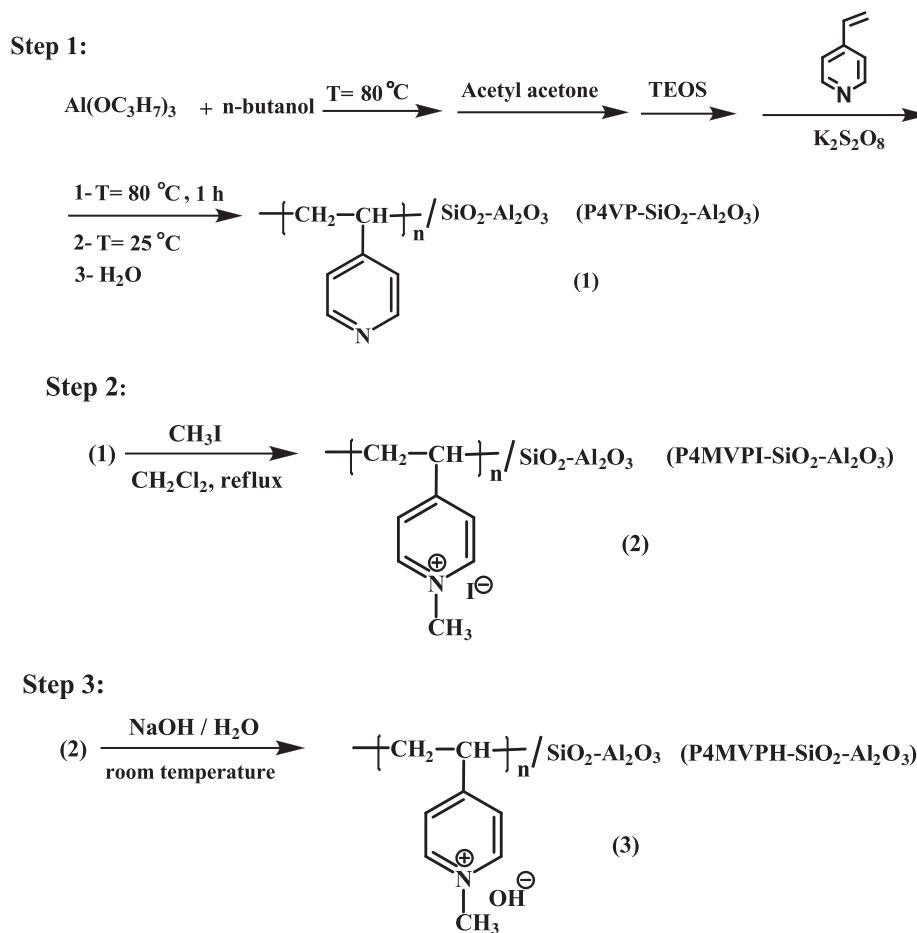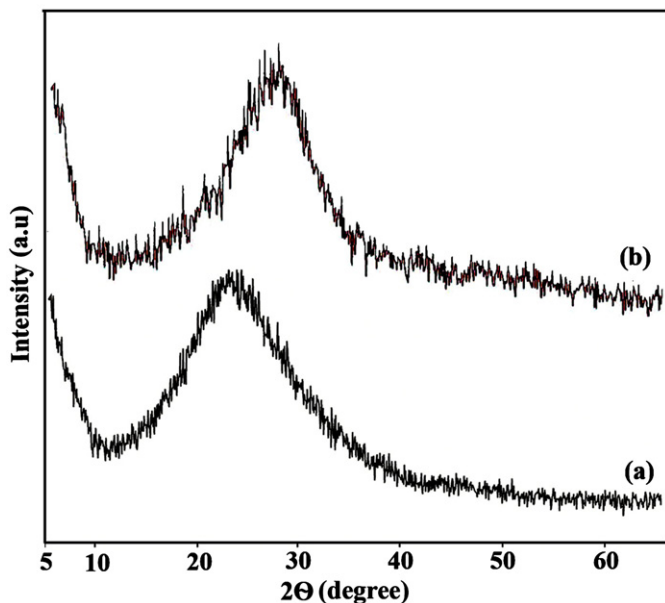### 3.1. Characterization of the catalyst

3.1.1. X-ray diffraction analysis

Fig. 1 depicts the powder X-ray diffraction patterns of the solids SiO$_2$–Al$_2$O$_3$ (a) and P4MVPH–SiO$_2$–Al$_2$O$_3$ (in-situ) (b). The solid SiO$_2$–Al$_2$O$_3$ displays the characteristic spectral profile of an amorphous aluminosilicate with an amorphous halo present in the $2\theta = 23$ [40]. This typical halo results from the dispersion of the angles and bond distances between the basic structural units (silicates and aluminates) which destroys the structure periodicity and produces a non-crystalline material. No changes in the diffraction patterns are observed of P4MVPH–SiO$_2$–Al$_2$O$_3$ (Fig. 1b), thus reinforcing the assumption that P4MVPH hybridization occurs on the solid surface without changing the structural form of the SiO$_2$–Al$_2$O$_3$.

3.1.2. FTIR analysis

Fig. 2 presents the FTIR spectra of SiO$_2$–Al$_2$O$_3$ (a), P4VP (b), P4VP–SiO$_2$–Al$_2$O$_3$ (c), P4MVPI–SiO$_2$–Al$_2$O$_3$ (d) and P4MVPH–SiO$_2$–Al$_2$O$_3$ (e). In the case of solid SiO$_2$–Al$_2$O$_3$, the bands expected for the aluminosilicate can be observed in the 1050 cm^{-1} (Si–O bond stretching) and 460 cm^{-1} (Al–O bond stretching) regions [41], which are seen in Fig. 1a,c,d,e. The other absorption peak of Al–O stretching vibration in the range of 1000–1200 cm^{-1} could not be resolved due to its overlap with the absorption peak of Si–O–Si stretching vibration in the range of 1000–1200 cm^{-1}. There is also a band in 3429 and 1632 cm^{-1} due to the O–H bonds vibration.

In the FT-IR spectrum of P4VP–SiO$_2$–Al$_2$O$_3$ (Fig. 1c), the new bands at 1598, 1558, 1496 and 1406 cm^{-1} were the characteristic absorptions of pyridine ring. Among them, the band which appeared at 1598 cm^{-1} was the stretching vibration absorption of C–N bond and the bands at 1558, 1496 and 1406 cm^{-1} were

Step 1:

$$Al(OC_3H_7)_3 \ + \ n\text{-butanol} \xrightarrow{\ T=80\,^{\circ}C\ } \xrightarrow{\ Acetyl\ acetone\ } \xrightarrow{\ TEOS\ } \xrightarrow{\ K_2S_2O_8\ }$$

$$\xrightarrow[\substack{2\text{- }T=25\,^{\circ}C \\ 3\text{- }H_2O}]{1\text{- }T=80\,^{\circ}C,\ 1\ h} \ \ \left[CH_2-CH\right]_n\big/ SiO_2\text{-}Al_2O_3 \quad (P4VP\text{-}SiO_2\text{-}Al_2O_3) \tag{1}$$

Step 2:

$$(1) \xrightarrow[CH_2Cl_2,\ reflux]{CH_3I} \ \left[CH_2-CH\right]_n\big/ SiO_2\text{-}Al_2O_3 \quad (P4MVPI\text{-}SiO_2\text{-}Al_2O_3) \tag{2}$$

Step 3:

$$(2) \xrightarrow[room\ temperature]{NaOH\ /\ H_2O} \ \left[CH_2-CH\right]_n\big/ SiO_2\text{-}Al_2O_3 \quad (P4MVPH\text{-}SiO_2\text{-}Al_2O_3) \tag{3}$$

Scheme 1. Preparation of P4MVPH–SiO$_2$–Al$_2$O$_3$.

Fig. 1. The powder XRD pattern of the solids (a) SiO$_2$–Al$_2$O$_3$ and (b) P4MVPH–SiO$_2$–Al$_2$O$_3$ (in-situ).

attributed to the stretching vibration absorption of C=C bond. Moreover, the presence of peaks at around 2800–3050 cm^{-1} corresponded to the aromatic and aliphatic C–H stretching in

P4VP–SiO$_2$–Al$_2$O$_3$. These were consistent with the spectrum of P4VP (Fig. 1b).

The appearance of the above bands shows that P4VP has been attached on the surface of SiO$_2$–Al$_2$O$_3$ and the P4VP–SiO$_2$–Al$_2$O$_3$ composite is obtained. In the spectra of P4MVPI–SiO$_2$–Al$_2$O$_3$ and P4MVPH–SiO$_2$–Al$_2$O$_3$ (Fig. 1d, e), a new peak appears at 1643 cm^{-1} which is ascribed to the C–N (CH$_3$–pyridinium) bond absorption. This observation confirms the N-alkylation of pyridine ring. In the FT-IR spectrum of P4MVPH–SiO$_2$–Al$_2$O$_3$ (Fig. 1e), the peak at 3450 cm^{-1} is stronger than in the other spectra, in which the stretching vibration of OH groups is shown. Furthermore, OH bending characteristic at 1643 cm^{-1} is seen. The appearance of these bands suggests that the exchange between OH$^-$ and I$^-$ groups on P4MVPI–SiO$_2$–Al$_2$O$_3$ occurred and the modified particles P4MVPH–SiO$_2$–Al$_2$O$_3$ were formed.

3.1.3. BET surface area and pore size analysis

The N$_2$ adsorption-desorption isotherms and the pore-size distributions of pure SiO$_2$–Al$_2$O$_3$ (a) and P4MVPH–SiO$_2$–Al$_2$O$_3$ (in-situ) (b) samples are shown in Fig. 3. The isotherms are similar to Type III isotherm with H1-type hysteresis loops at high relative pressure according to the IUPAC classification, characteristic of amorphous and microporous materials. The specific surface area and the pore size have been calculated using Brunauer–Emmett–Teller (BET) and Barrett–Joyner–Halenda (BJH) methods, respectively.

The structure data of all these materials (BET surface area, total pore volume, and pore size) are summarized in Table 1. It is known that SiO$_2$–Al$_2$O$_3$ has a high BET surface area (178 m^2/g),
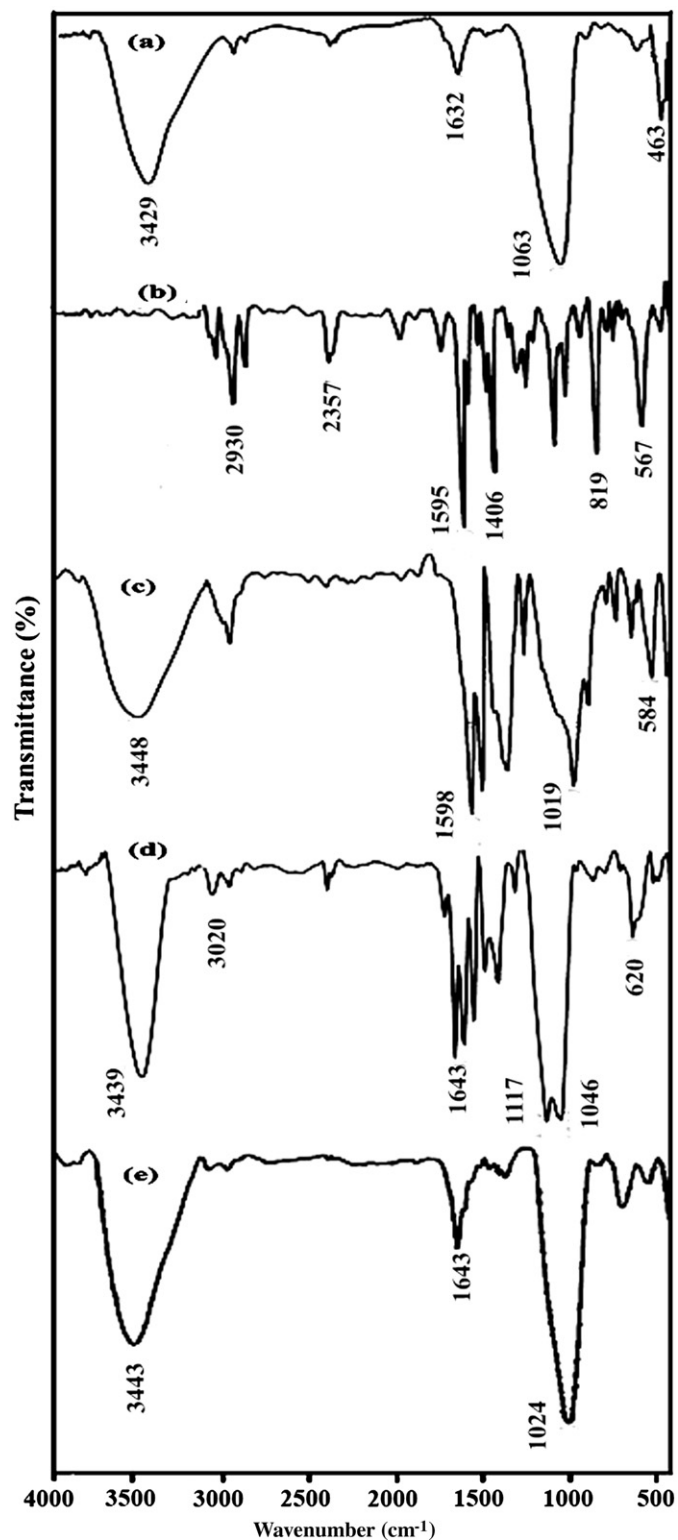
Fig. 2. FT-IR spectra of (a) SiO_2–Al_2O_3, (b) P4VP, (c) P4VP–SiO_2–Al_2O_3, (d) P4MVPI–SiO_2–Al_2O_3 and (e) P4MVPH–SiO_2–Al_2O_3.

Fig. 3. The N_2 adsorption-desorption isotherm of pure (a) SiO_2–Al_2O_3 and (b) P4MVPH–SiO_2–Al_2O_3 (in-situ) and pore-size distributions of (c) SiO_2–Al_2O_3 and (d) P4MVPH–SiO_2–Al_2O_3 (in-situ).

Table 1
Porosity data of SiO_2–Al_2O_3 and P4MVPH–SiO_2–Al_2O_3 samples.

Sample	BET surface area ($m^2 g^{-1}$)	Pore volume ($cm^3 g^{-1}$)	Pore size (nm)
SiO_2–Al_2O_3	178.0	1.5	33.6
P4MVPH–SiO_2–Al_2O_3	89.3	0.6	27.0
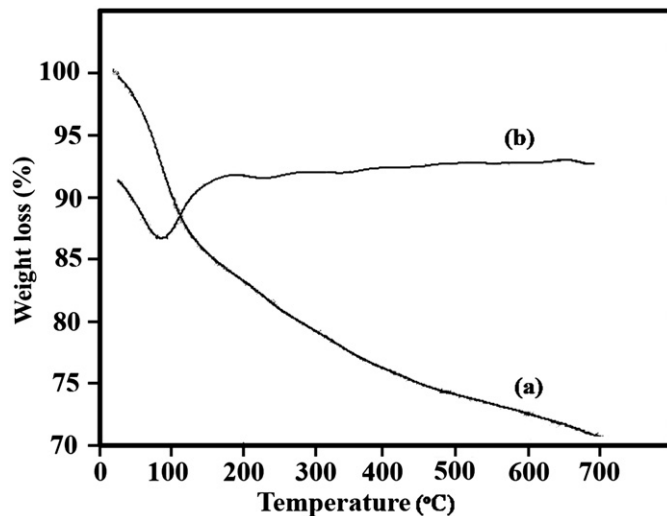
Fig. 4. TGA curves of (a,b) P4MVPH–SiO_2–Al_2O_3 (in-situ).

a large pore volume (1.49 cm^3/g) and a pore size (33.64 nm), indicative of its potential application as a host in organic materials. Also, Table 1 shows that after hybridization with P4MVPH through in-situ polymerization, textural properties of composite are smaller than SiO_2–Al_2O_3 support.

The pore size distribution patterns shown in Fig. 3c,d, reveal that the homogeneous distribution of polymer could block small pores of SiO_2–Al_2O_3 or could be well-dispersed in inner pore resulting in a decrease in surface area and average pore diameter (Fig. 3d). However, for the catalyst prepared by in-situ method, the polymer chains are entangled like skeins in the structure of SiO_2–Al_2O_3, and lead to increase the contact surface.

3.1.4. Thermal property

The thermogravimetric analysis (TG and DTG) curve of the P4MVPH–SiO_2–Al_2O_3 has been investigated. The P4MVPH–SiO_2–Al_2O_3 (in-situ) sample (Fig. 4) shows two separate weight loss

steps. The first step (around 13%, w/w) appearing at temperature $< 150\,^{\circ}C$ corresponded to desorption of physically adsorbed water (i.e., adsorbed water on the inner and outer surface). The second weight loss (about 150–700 °C) which amounts to around 17% (w/w) is related to the decomposition of the polymer moiety.

3.1.5. Scanning electron microscopy (SEM)

Fig. 5 gives the scanning electron microscopy (SEM) photographs of SiO_2–Al_2O_3 (a,c) and P4MVPH–SiO_2–Al_2O_3 (in-situ) (b,d) samples.

In the SEM photograph of SiO_2–Al_2O_3, it can be seen that the mixed-oxide surface is uniform and is like a sponge (Fig. 5a,c). On the other hand, Fig. 5b,d shows a different morphology. The SEM photograph of P4MVPH–SiO_2–Al_2O_3 (in-situ) shows regular distribution of P4MVPH in the structure of SiO_2–Al_2O_3. It can be seen that P4MVPH is completely mixed with SiO_2–Al_2O_3 particles and the composite is uniform. It is obvious that before hybridization, the surface of SiO_2–Al_2O_3 is somewhat smooth, whereas after hybridization, the surface of composite becomes coarser. In addition, it can be seen that the particle size in the P4MVPH–SiO_2–Al_2O_3 is much lower than that of SiO_2–Al_2O_3 (Fig. 5c,d).

3.2. Catalytic activity

This novel composite was synthesized and fully characterized with different methods. The main goal of this catalytic synthesis was to compare this organic–inorganic composite with other functional polymeric materials and to expand the use of these types of composites for organic reactions. This composite was prepared by a very simple and inexpensive method without using any bridged organosilanes compound (the bridged organosilanes precursors either involve complicated synthesis and purification method or are very expensive). In order to investigate the basic properties of this catalyst, the Knoevenagel condensation was chosen as a typical reaction.

The accepted mechanism for the base-catalyzed Knoevenagel condensation involves a first step in which the formation of the carbanion on the methylenic group occurs by abstraction of the proton by the basic catalyst. This is followed by attack of the carbanion intermediate to the carbonyl group. Finally, elimination of the hydroxyl group occurs to form a C=C bond and water, while the basic site (hydroxide ion) is restored. Plausible mechanism of the Knoevenagel reaction over P4MVPH–SiO_2–Al_2O_3 is denoted in Scheme 2.

The effects of some parameters on Knoevenagel condensations of benzaldehyde with malononitrile were investigated, and the results are as follows:

The effect of the amount of catalyst on the Knoevenagel condensation reaction was investigated using 1 mmol of benzaldehyde and 1 mmol of malononitrile at room temperature and in solvent-free conditions. The values are shown in Table 2. The results showed that by increasing the amount of catalyst from 0.06 to 0.12 g, the reaction completion time decreased. When 0.12 g of the catalyst was employed, the reaction was completed in less than 3 min at room temperature. Moreover, with an increase or a decrease in the catalyst amount, the selectivity was constant.

The effect of the amount of 4-vinyl pyridine (4VP) on the yield of the reaction was studied by varying the amount of monomer, where the other parameters were kept constant (Table 3). By increasing the amount of monomer to 2 mL (the amounts of aluminum isopropoxide and TEOS were kept constant according to the experimental section), the yield increased because of the increase in the basic active catalyst sites. With further increase in monomer amount from 2 to 3 mL, the completion time increased, which can be due to aggregation of the polymers.

In order to investigate the effect of SiO_2–Al_2O_3 on the catalytic activity, in the absence of P4MVPH, SiO_2–Al_2O_3 was used as the catalyst for the Knoevenagel reaction and after 30 min, yield was 7% (Table 3). However, the yield of the Knoevenagel reaction over P4MVPH–SiO_2–Al_2O_3 was 98% in 3 min (in the modified conditions). As we showed in the plausible mechanism (Scheme 2), the hydroxide ions are the active sites of the catalyst. These active sites do not exist in the SiO_2–Al_2O_3 and the basic sites in P4MVPH–SiO_2–Al_2O_3 are more active than SiO_2–Al_2O_3. Thus the higher activity of P4MVPH–SiO_2–Al_2O_3 in the Knoevenagel reaction was not attributed to the higher surface area (Table 1), and it should be related to the nature of the active basic sites. Also comparative reaction by using P4MVPH and P4MVPH–SiO_2–Al_2O_3
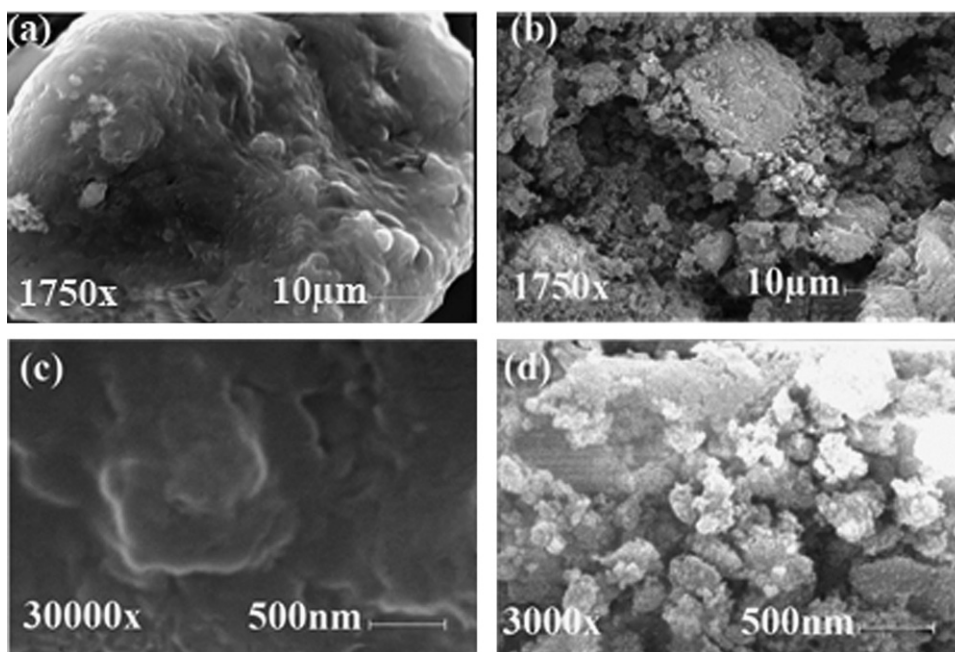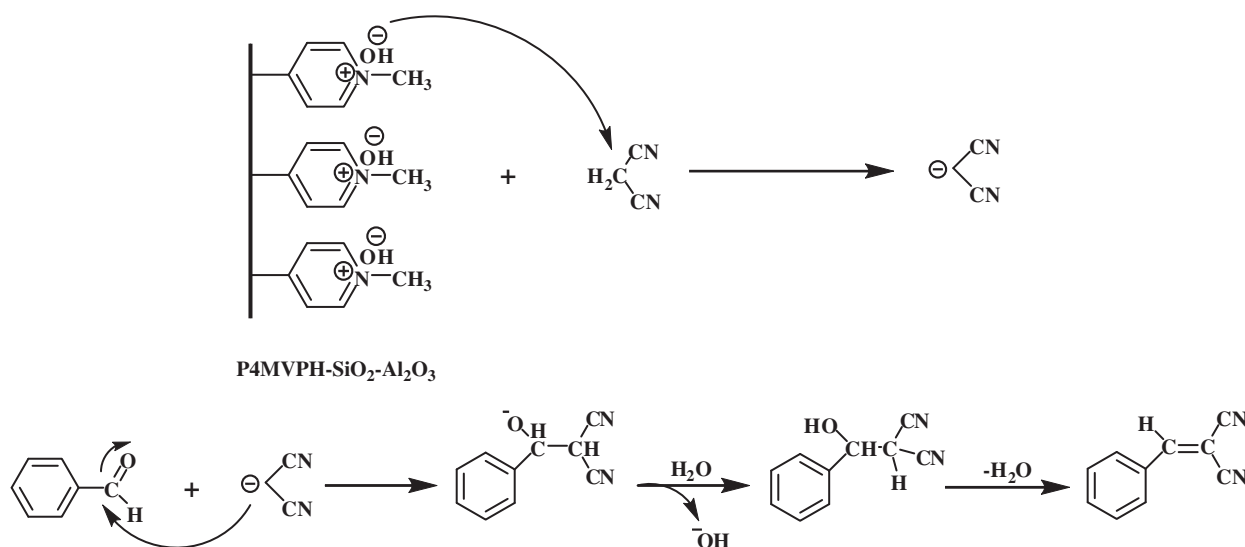

Fig. 5. Scanning electron microscopy (SEM) photographs of (a,c) SiO_2–Al_2O_3 and (b,d) P4MVPH–SiO_2–Al_2O_3 (in-situ).

Scheme 2. Plausible mechanism of the Knoevenagel reaction over P4MVPH–SiO$_2$–Al$_2$O$_3$.

Table 2
Effect of the amount of catalyst[a].

Amount of catalyst (g)	Time (min)	Yield (%)[b]
0.06	3	45
	8	98
0.08	3	50
	6	98
0.1	3	85
	4	98
0.12	3	98

[a] Reaction conditions: benzaldehyde (1 mmol), malononitrile (1 mmol), catalyst (0.12 g, P4MVPH–SiO$_2$–Al$_2$O$_3$), solvent-free, room temperature.
[b] Isolated yield.

Table 3
Effect of 4-VP amount on catalytic activity of P4MVPH–SiO$_2$–Al$_2$O$_3$ [a].

Amount of 4-VP (mL)[b]	Time (min)	Yield (%)[c]	Amount of basic sites of the catalyst (mmol g^{-1})
–	30	7	–
1	3	60	2.6
	7	98	
2	3	98	4.8
3	3	80	5.6
	5	98	

[a] Reaction conditions: benzaldehyde (1 mmol), malononitrile (1 mmol), catalyst (0.12 g, P4MVPH–SiO$_2$–Al$_2$O$_3$), solvent-free, room temperature.
[b] The amounts of Aluminum isopropoxide and TEOS were kept constant according to the experimental section.
[c] Isolated yield.

Table 4
Reusability of the catalyst[a].

Cycle	Time (min)	Yield (%)[b]
Fresh	3	98
1	3	95
	4	98
2	3	85
	5	98
3	3	60
	6	98
4	3	45
	8	98
5	3	40
	9	98

[a] Reaction conditions: benzaldehyde (1 mmol), malononitrile (1 mmol), catalyst (0.12 g, P4MVPH–SiO$_2$–Al$_2$O$_3$), solvent-free, room temperature.
[b] Isolated yield.

area on whose surfaces polymer chains can be distributed uniformly. In this condition, the quternized pyridine rings that are the original centers for doing the reaction, are free and it is possible for the reactant to reach the active sites of the catalyst (hydroxide ions). So, we can conclude that the yield of the reaction was high on the surface of P4MVPH–SiO$_2$–Al$_2$O$_3$. On the other hand, in the P4MVPH there are many interactions between the chains of the polymers and some of the pyridine ring trapped in the chains of the polymer. So, there is hindrance around the pyridine rings that can prevent the reactant to reach the active sites of the catalyst (hydroxide ions). This can reduce the activity of the P4MVPH. Therefore, it can be said that the existence of both organic and inorganic phases has critical effects on the catalytic activity of the catalyst.
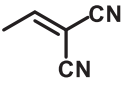
The reusability of the catalyst was studied by using P4MVPH–SiO$_2$–Al$_2$O$_3$ in recycling experiments (Table 4). In order to regenerate the catalyst, after the completion of the reaction, it was separated by filtration, washed several times with deionized water, dried at 60 °C and used in the reaction with a fresh reaction mixture. The catalyst was reused up to 5 times without any significant loss of its catalyst activity, and the selectivity was constant (100%).

The P4MVPH–SiO$_2$–Al$_2$O$_3$ catalyst also showed good activity and selectivity in the Knoevenagel condensation reaction using

showed that P4MVPH–SiO$_2$–Al$_2$O$_3$was more efficient, by completion the reaction in a short time. On the other hand, the yield was decreased and the reaction was carried out in a long period of time using P4MVPH (81% yield after 20 min).

It should be mentioned that one of the greatest advantages of this catalyst was to easily use due to its powdery structure. P4MVPH was adhesive and this character made it hard to separate it from the vessel; but after in-situ hybridization with SiO$_2$–Al$_2$O$_3$ and making P4MVPH–SiO$_2$–Al$_2$O$_3$ composite, it becomes powdery which was easily used and recycled. SiO$_2$–Al$_2$O$_3$ has high surface

Table 5
Knoevenagel condensation of various aldehydes and malononitrile catalyzed by P4MVPH–SiO$_2$–Al$_2$O$_3$[a]
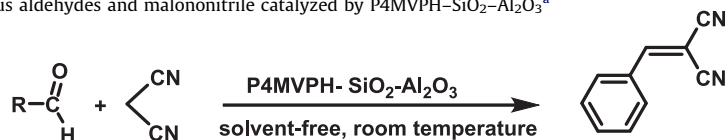
Entry	Substrate	Product	Time (min)	Yield (%) [b]	Mp (deg.)		Ref.
					Found	Reported	
1			3	98	81–83	82–84	[42,46,47]
2[c]			8	98	81–83	82–84	[42,43,47]
3			15	98	182–183	180–182	[43]
4[c]			24	98	182–183	180–182	[43]
5			28	98	160–162	159–161	[42,43,47]
6[c]			40	98	160–162	159–161	[42,43,47]
7			20	98	96–98	95–96	[45,47]
8			15	98	114–118	116–117	[48]
9			16	98	153–154	153–155	[44]
10[c]			28	98	153–154	153–155	[44]
11			24	98	167–168	168–169	[42,43,47]
12			30	98	175–179	178–180	[47]
13			27	98	132–134	133–135	[31]
14			5	98	102–104	103–104	[47]
15			90	91	Liquid	–	[31]
16			55	98	Liquid	–	[31]

Table 5 (continued)

Entry	Substrate	Product	Time (min)	Yield (%) [b]	Mp (deg.)		Ref.
					Found	Reported	
17			40	98	Liquid	–	[32]

[a] Reaction conditions: aldehyde (1 mmol), malononitrile (1 mmol), catalyst (0.12 g, P4MVPH–SiO$_2$–Al$_2$O$_3$), solvent-free, room temperature.
[b] Isolated yield.
[c] Catalyst (0.06 g, P4MVPH–SiO$_2$–Al$_2$O$_3$).

different kinds of aromatic and aliphatic aldehydes [42–48]. The results are given in Table 5. In all cases, selectivity for carbonyl compound was 100%.

4. Conclusion

In summary, it was demonstrated that P4MVPH–SiO$_2$–Al$_2$O$_3$ as a novel basic polymeric composite could behave as a recyclable catalyst for the Knoevenagel condensation reaction of various aldehydes with malononitrile with 100% selectivity to α,β-unsaturated carbonyl compounds offering a good yield and also high chemo-selectivity. The reactions occur at room temperature and give excellent yields of the products. The catalyst could be easily recovered by simple filtration and washing, and could be reused up to 5 times without significant loss in its catalytic activity. Therefore, it is believed that the new synthetic method reported here would greatly contribute to an environmentally greener and safer process.

References

[1] H. Wang, M. Wang, N. Zhao, W. Wei, Y. Sun, Catal. Lett. 105 (2005) 253–257.
[2] M. Ai, Appl. Catal. A: Gen. 288 (2005) 211–215.
[3] X. Liu, H. He, Y. Wang, S. Zhu, Catal. Commun. 8 (2007) 1107–1111.
[4] F. Mammeri, E.L. Bourhis, L. Rozes, C.J. Sanchez, Mater. Chem. 15 (2005) 3787.
[5] H. Sugimoto, E. Nakanishi, K. Yamauchi, K. Daimatsu, T. Yasumura, K. Inomata, Polym. Bull. 52 (2004) 209–218.
[6] Y.G. Hsu, L.F. Chang, C.P. Wang, Mater. Sci. Eng. A 367 (2004) 205–217.
[7] K.-M. Kim, K. Adachi, Y. Chujo, Polymer 43 (2002) 1171–1175.
[8] G. Liu, H. Zhang, X. Yang, Y. Wang, Polymer 48 (2007) 5896–5904.
[9] A.P. Wight, M.E. Davis, Chem. Rev. 102 (2002) 3589–3614.
[10] J. Evans, A.B. Zaki, M.Y. El-Sheikh, S.A. El-Safty, J. Phys. Chem. B 104 (2000) 10271–10281.
[11] J. Kramer, A.R. Garcia, W.L. Driessen, J. Reedijk, Chem. Commun. (2001) 2420–2421.
[12] A. Walcarius, M. Etienne, J. Bessiere, Chem. Mater. 14 (2002) 2757–2766.
[13] R. Voss, A. Thomas, M. Antonietti, G.A. Ozin, J. Mater. Chem. 15 (2005) 4010.
[14] S. Yoo, J.D. Lunn, S. Gonzalez, J.A. Ristich, E.E. Simanek, D.F. Shantz, Chem. Mater. 18 (2006) 2935–2942.
[15] M.E. Davis, A. Katz, W.R. Ahmad, Chem. Mater. 8 (1996) 1820–1839.
[16] R.J. Kalbasi, M. Kolahdoozan, A. Massah, K. Shahabian, Bull. Korean Chem. Soc 31 (2010) 2618–2626.
[17] R.J. Kalbasi, M. Kolahdoozan, K. Shahabian, F. Zamani, Catal. Commun. 11 (2010) 1109–1115.
[18] I. Zareba-Grod, W. Mista, W. Strek, E. Bukowska, K. Hermanowicz, K. Maruszewski, Opt. Mater. 26 (2004) 207–211.
[19] M. Monroy-Barretoa, J.C. Aguilara, E.R.d.S. Miguel, A.L. Ocampoa, M. Munob, J.d. Gyvesa, J. Membr. Sci. 344 (2009) 92–100.
[20] F. Mammeri, L. Rozes, E.L. Bourhis, C. Sanchez, J. Eur. Ceram. Soc. 26 (2006) 267–272.
[21] H. Kabashima, H. Tsuji, T. Shibuya, H. Hattori, J. Mol. Catal. A 155 (2000) 23–29.
[22] P. Leelavathi, S.R. Kumar, J. Mol. Catal. A: Chem. 240 (2005) 99–102.
[23] R.M. Kumbhare, M. Sridhar, Catal. Commun. 9 (2008) 403–405.
[24] J. Bennazha, M. Zabouily, S. Sbeti, A. Boukhari, E.M. Holt, Catal. Commun. 2 (2001) 101–104.
[25] M. Zhang, A.Q. Zhang, X.H. Tang, Chin. J. Org. Chem. 24 (2004) 1106–1107.
[26] X.M. Xu, Y.Q. Li, M.Y. Zhou, Chin. J. Org. Chem. 24 (2004) 1253–1256.
[27] H. Yi, C. Jue, G.L. Zhang, Synth. Commun. 35 (2005) 739.
[28] Y. Kubota, Y. Nishizaki, H. Ikeya, M. Saeki, T. Hida, S. Kawazu, M. Yoshida, H. Fujii, Y. Sugi, Micropor. Mesopor. Mater. 70 (2004) 135–149.
[29] S. Wada, H. Suzuki, Tetrahedron Lett. 44 (2003) 399–401.
[30] X. Zhang, E.S.M. Lai, R. Martin-Aranda, K.L. Yeung, Appl. Catal. A: Gen. 261 (2004) 109–118.
[31] B.M. Reddy, M.K. Patil, K.N. Rao, G.K. Reddy, J. Mol. Catal. A: Chem. 258 (2006) 302–307.
[32] S. Mallouk, K. Bougrin, A. Laghzizil, R. Benhida, Molecules 15 (2010) 813–823.
[33] N. Taha, Y. Sasson, M. Chidambaram, Appl. Catal. A: Gen. 350 (2008) 217–224.
[34] F.A. Khan, F.J. Dash, R. Satapathy, S.K. Upadhyay, Tetrahedron Lett. 45 (2004) 3055–3058.
[35] B.M. Choudary, M.L. Kantam, V. Neeraja, K.K. Rao, Green Chem. 3 (2001) 257–260.
[36] X.S. Wang, J.T. Li, W.Z. Yang, T.S. Li, Ultrason. Sonochem. 9 (2002) 159–163.
[37] L. Martins, W. Hölderich, P. Hammer, D. Cardoso, J. Catal. 271 (2010) 220–227.
[38] K.M. Parida, S. Mallick, P.C. Sahoo, S.K. Rana, Appl. Catal. A: General 381 (2010) 226–232.
[39] T. Seki, M. Onaka, J. Mol. Catal. A: Chem. 263 (2007) 115–120.
[40] M. Ghiaci, B. Rezaei, R.J. Kalbasi, Talanta 73 (2007) 37–45.
[41] G.S. Machado, K.A.D.F. Castroa, O.J. Lima, E.J. Nassarb, K.J. Ciuffib, S. Nakagaki, Colloid Surf. A: Physicochem. Eng. Aspects 349 (2009) 162–169.
[42] G. Postole, B. Chowdhury, B. Karmakar, K. Pinki, J. Banerji, A. Auroux, J. Catal. 269 (2010) 110–121.
[43] S.D. Sharma, P. Gogoi, D. Konwar, Indian J. Chem. 46 (2007) 1672–1678.
[44] C. Yue, A. Mao, Y. Wei, M. Lu, Catal. Commun. 9 (2008) 1571–1574.
[45] M. Gupta, R. Gupta, M. Anand, Beilstein J. Org. Chem. 5 (2009) 68.
[46] A. Kumar, M. Dewan, A. Saxena, A. De, S. Mozumdar, Catal. Commun. 11 (2010) 679–683.
[47] M. Hosseini-Sarvari, H. Sharghi, S. Etemad, Chin. J. Chem. 25 (2007) 1563–1567.
[48] F. Santamarta, P. Verdia, E. Tojo, Catal. Commun. 9 (2008) 1779–1781.